EFFECTS OF EXTERNAL COOLED EGR ON PARTICLE NUMBER EMISSIONS UNDER COLD AND WARM SPARK IGNITION DIRECT INJECTION ENGINE CONDITIONS

by

Jie LIU**, Shaohua SUN, and Caizhou XU

Pan Asia Technical Automotive Center, Shanghai, China

Original scientific paper
https://doi.org/10.2298/TSCI180207119L

External cooled exhaust gas recirculation (EGR) is drawing significant attention in downsized boosted spark ignition direct injection (SIDI) engines due to its potential to improve fuel economy. Meanwhile, worldwide emission standards pressure to reduce particle number (PN) emissions is generating great challenges for SIDI engine development. Thus it is necessary to examine the PN emission behaviors when implementing cooled EGR as a fuel-saving technology. In this study, the low-load with cold-engine (40 °C and 60 °C coolant temperature) and high-load with warm-engine (90 °C coolant temperature), representing high particle emission engine operating conditions over new European driving cycle, were chosen to understand the effects of cooled EGR on PN emissions in a downsized boosted SIDI gasoline engine using Horiba MEXA SPCS1000 PN measurement instrument. Measurements indicate that increasing cooled EGR levels provide higher PN emissions at low-load cold-engine operation, however, lower PN emissions at high-load warm-engine operation. This study, therefore, provides insight how cooled EGR impacts PN emissions under cold and warm engine operation.

Key words: *particle number, exhaust gas recirculation, cold engine, warm engine, fuel consumption, spark ignition direct injection*

Introduction

Worldwide pressure to reduce automotive fuel consumption is driving the introduction of a number of new gasoline engine technologies [1]. One of the most promising concepts currently is the downsized boosted SIDI engine, providing better fuel economy and higher specific power output in gasoline engines, and is increasing its market share relative to port fuel injection (PFI) [2-4]. For example, PFI equipped light-duty vehicles accounted for over 99% of light-duty vehicles sold in the United States each year between 1996 and 2007 [5]. After 2007, SIDI engines began to rapidly enter the U. S. market, accounting for 3.1% light-duty vehicles in 2008, 18.4% in 2011 and increasing to 46.4% in 2015 [6]. In the European automotive market, overall share of SIDI vehicles increased sharply beginning in 2008, and is estimated at around 35% in 2014 [7]. However, It is well known that the PN and particle mass emissions from SIDI engine are higher than that from PFI engine, both at steady-state and driving cycle conditions [8, 9]. The increase in particle emissions can be mainly attributed to three types of rich combustion: (1) locally fuel-rich mixture in the combustion chamber, (2) diffusion-controlled burning

* Corresponding author, e-mail: jie_liu@patac.com.cn

of thin films of liquid fuel on the piston or cylinder wall, called *pool fires*, and (3) diffusion flames in the vicinity of the injector tip, during and/or after the final phase of completion of the normal combustion event [10-13].

Increasingly stringent emission standards are also drawing great attention on particle emissions from SIDI engines. In Europe, a particle mass limit of 5 mg/km for SIDI powered vehicles was introduced for the first time in EU5a. From 2014, a PN limit of $6.0 \cdot 10^{12}$ particles per km, over the new European driving cycle (NEDC) for SIDI powered vehicles has been applied, and the PN limit will be further tightened to $6.0 \cdot 10^{11}$ particles per km, with the introduction of EU6c legislation in September 2017 [14]. Furthermore, the new driving cycle, worldwide harmonized light duty test cycle (WLTC), will be introduced in EU6c [12]. Compared to NEDC, WLTC includes more amounts of non-urban driving phases and more aggressive acceleration levels, which has the potential to increase particle emissions [12]. For current commercial SIDI engines, it is relative easier to meet the EU6c particle mass limitation of 4.5 mg/km [15, 16]. However, additional efforts for further reducing PN emissions are required to satisfy EU6c PN regulation of $6.0 \cdot 10^{11}$ particles per km [15, 16]. Previous researches has documented that the highest PN emissions over NEDC and WLTC driving cycles are from cold engine operation, including cold start, catalyst heating phase, and acceleration [12, 15, 16]. In addition, the low engine speed weakens the level of charge motion as compared with high engine speed. This results in poor mixture preparation due to reduced fuel evaporation and mixture homogeneity, which is another factor for high particle emissions. Therefore, the engine speed of 1400 rpm and cold engine (40 °C and 60 °C engine coolant temperature) at 6 bars brake mean effective pressure (BMEP) was chosen to investigate in this study. Even through, the cold engine operation accounts for the most part of particle emissions over driving cycle, the high-load and acceleration process at warm engine operation are more and more relevant to meet PN emissions limits, especially for downsized boosted SIDI engines. Hence, the warm engine operating condition (90 °C engine coolant temperature) for the investigation in this study was selected at 2200 rpm and 10 bar BMEP.

External cooled EGR has been demonstrated to be one of the effective strategies to achieve the low temperature combustion condition in compression ignition engines [17]. In boosted spark ignition engines, cooled EGR shows the potential to improve fuel economy by between 5% and 30% with the largest improvements occurs at typical fuel enrichment regions (high-speed high-load conditions) [18]. At low load conditions, the better fuel economy by cooled EGR is mainly attributed to reduced heat losses, reduced pumping working, and higher ratio of specific heats [19]. For knock-limited high-load conditions, suppressed knock plays a dominant role in the improved fuel economy, followed by the reduced heat losses [19]. At fuel enrichment conditions, the most important contributing factors for the improvement in fuel economy is the reduced amount of required fuel enrichment due to decreased exhaust gas temperature and suppressed knock [18, 19]. Cooled EGR also leads to lower NO_x emissions with somewhat higher HC emissions, which have been well documented in previous studies [20-22]. Hedge *et al*. [23] presented the experimental research in a SIDI gasoline engine and concluded that both PN and soot mass emissions can be reduced by cooled external EGR at medium-load (more than 6 bar BMEP) and high power enrichment region (16 bar BMEP and 3000 rpm) conditions. Su *et al*. [24] investigated the effect of cooled EGR on soot emissions for a 2.0 L turbocharged SIDI engine at high and full load conditions, and indicated that approximately 20% cooled EGR has the potential to reduce filtered-smoke number by as much as 50%. More recent work in a 1.2 L turbocharged SIDI engine illustrated that 12% cooled EGR reduces PN emissions by 6% at a knock-limited high-load condition (2000 rpm, 11 bar BMEP) [25].

Prior studies provide some insight into understanding how cooled EGR impacts fuel consumption and gas emissions in gasoline SIDI engines. However, there appears to be less information available on PN behaviors with cooled EGR in SIDI engines, especially at cold engine operation, which is of particular interest for particle emissions as discussed above. The objective of the present work is to explore the effect of cooled EGR on PN emissions in a boosted SIDI engine operated at low-load cold-engine and high-load warm-engine conditions, representing high particle emission engine operating conditions over NEDC.

Experimental details

Engine

A 1.4 L boosted gasoline SIDI engine is equipped with a high pressure cooled EGR system to investigate the effect of cooled EGR on PN emissions and fuel consumptions under cold and warm engine conditions. Engine specifications are provided in tab. 1. This high pressure DI injectors are located close to the center of combustion chamber (central injection) with an operating range up to 20 MPa. A dual independent variable valve timing (VVT) and a production fixed-geometry twin-scroll turbocharger with a pneumatically controlled wastegate are used with this engine. EGR is transported from upstream of the three-way catalyst and introduced into the intake manifold system. An EGR cooler is used to lower the exhaust temperature to below 100 °C. An intercooler controls intake temperature to 38 ± 1 °C.

Table 1. Engine specifications

Displacement	1.4 L
Bore	74 mm
Stroke	81.5 mm
Compression ratio	10
Fuel system	Direct injection (Central)
Boosting system	Twin-scroll turbocharger
Valve train	Dual independent VVT

An AVL AC dynamometer system is used to maintain desired engine speed. As shown in fig. 1 an AVL 733s fuel system and an AVL 753C fuel temperature control system provide accurate fuel delivery conditions. The AVL Puma control and data acquisition system interfaced with the facility and engine instrumentation were used to collect and process the data.

Kistler 6125C piezoelectric in-cylinder pressure transducers are employed and data are processed by a high-speed data acquisition system at a resolution of 0.1 crank angle degree (CAD) for 300 consecutive engine cycles at each operating point.

Emission measurement

In this study, the PN concentration was measured by Horiba MEXA-1000SPCS. As shown in fig. 1, engine exhaust was sampled directly from post-three-way catalyst (TWC), followed by a heated sampling line maintained at 191 ± 7 °C, a pre-dilution unit (PDU), a particle transfer tubing maintained at 47 ± 5 °C, a particle pre-classifier (PCF), and a volatile particle remover (VPR) upstream of a laser-based condensation particle counter (CPC). The PDU firstly diluted the sample with a dilution ratio of 10:1. Larger particles with diameter greater than 2.5 μm were removed by the particle pre-classifier. The VPR was designed to suppress particle nucleation within the sample and remove the soluble organic fraction (SOF) and sulfur component. The VPR comprises a particle number diluter (PND1), an evaporation tube (ET) and a second diluter (PND2) in series. The PND1 was operated at a (wall) temperature 150 ± 10 °C and a dilution ratio of 50:1. The evaporation tube was operated with a wall temperature 350 ± 10 °C. The PND2 was operated at a (wall) temperature 25 ± 1°C and a dilution ratio of 15:1. After VPR, the sample was introduced into CPC where butanol condensed onto

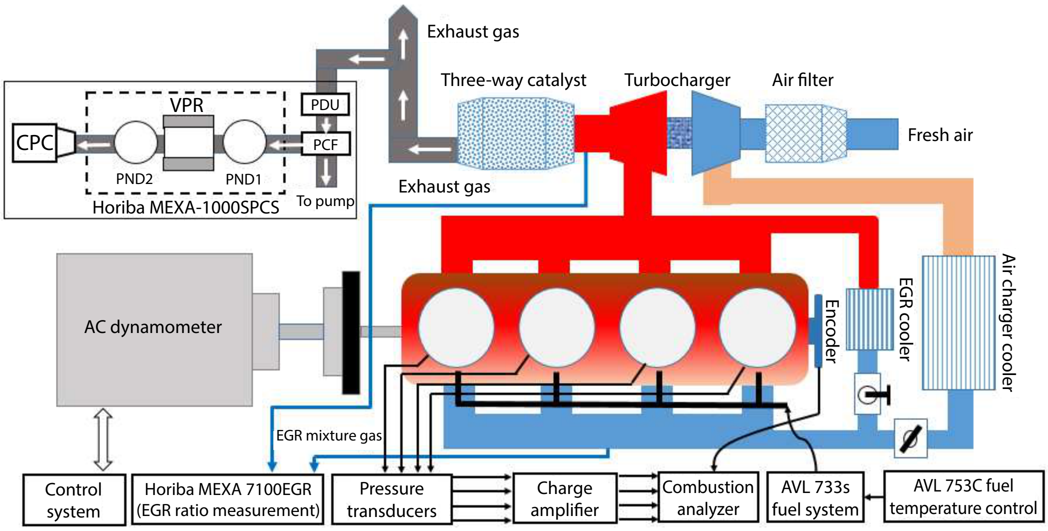

Figure 1. Schematic of particle counting system and EGR measurement

particles in the sample flow, creating droplets large enough to be detected efficiently using a light-scattering technique. Data are collected at a sampling rate of 10 Hz for 60 seconds. The PN tests for each EGR case are repeated by 3 times. The measured variability range of the 3 tests and averaged results are shown in this paper.

In order to evaluate the cooled EGR ratio, the CO_2 volume concentrations in the intake manifold and exhaust manifold are measured using Horiba MEXA 7100EGR. The EGR ratio is determined as the ratio of CO_2 measured in the engine intake to the CO_2 measured in the engine exhaust.

Operating conditions and test procedure

The engine is operated at 1400 rpm, 6 bar BMEP with cold engine operation (20 °C and 40 °C coolant temperature), and 2200 rpm, 10 bar BMEP with warm-engine (90 °C coolant temperature), representing high particle emission engine operating conditions over NEDC. At each engine operating condition, an EGR sweep test was conducted to examine the effect of cooled EGR on particle emissions and fuel consumption behaviors. To better isolate the effect of cooled EGR from other engine control parameters, air fuel ratio, fuel pressure, injection timing, intake and exhaust cam phasing, intake temperature, coolant temperature and oil temperature are kept constant during EGR sweeps, in which, fuel pressure, injection timing, intake and exhaust cam phasing were determined for minimum fuel consumption and particle emissions at cooled EGR rate 0%. Spark timing was optimized for each EGR case for minimum fuel consumption. For all the tests points, the engine was operated in the homogeneous-charge combustion mode at a stoichiometric air-fuel ratio. Table 2 summarizes the engine control parameters during the tests.

Engine simulation models

To better understand the particle behaviors with cooled EGR, the in-cylinder temperature was calculated by GT-Power® code (Gamma Technologies). The intake and exhaust system flows were modeled as 1-D fluid dynamics, considering varying cross section, friction, heat transfer and variable gas properties. Wiebe model was used to calculate combustion burn rate [26]. The cylinder heat transfer was calculated using the Woschni correlation [27]. Figures 2 and 3 shows a comparison of in-cylinder pressure trace between the experimental and calculated results at 1400 rpm, 6 bar BMEP engine operating condition without EGR, and 23% EGR, respectively.

The good agreement proves that the simulation model is accurate enough to capture the characteristics of gas exchange and combustion processes. Similarly good agreements were also obtained for other engine operating conditions as shown in tab. 2.

Table 2. Engine operating conditions

Engine	SIDI
Speed	1400 rpm
BMEP	6 bar
Injection pressure	12 MPa
Injection timing	300 °bTDC
Air fuel ratio	14.6
Intake valve open (IVO)	6.5 °aTDC at 0.5 mm lift
Exhaust valve close (EVC)	9 °aTDC at 0.5 mm lift
Intake temperature	38 ± 1 °C
Engine-out coolant temperature	40/60 ± 0.5 °C
Oil sump temperature	40/60 ± 0.5°C

Results and discussion

The role of cooled EGR on PN emissions and fuel consumption behaviors at low-load cold-engine operation and high-load warm-engine operation were examined under above mentioned test procedures.

Low-load cold-engine evaluation

The effect of cooled EGR on PN emissions at 1400 rpm, 6 bar BMEP under cold engine condition is examined in fig. 4. Two PN behaviors are observed: (1) PN emissions are increased when lowering coolant temperature from 60 °C to 40 °C, and this PN deterioration is realized throughout the HP-EGR range, and (2) PN emissions are increased when increasing HP-EGR level both at 60 °C and 40 °C coolant temperatures, and the PN increase amplitude with EGR is higher for 40 °C coolant temperature than 60 °C coolant temperature. For example, 27% EGR provides 40% higher PN emissions at 60 °C coolant temperature condition, and only 23% EGR generates 60% higher PN emissions at 40 °C coolant temperature condition.

The dependence of PN emissions on coolant temperature observed in fig. 4 is fundamentally determined by the effect of combustion chamber wall temperature on particle formation process. During the cold engine operation, combustion chamber wall is at a

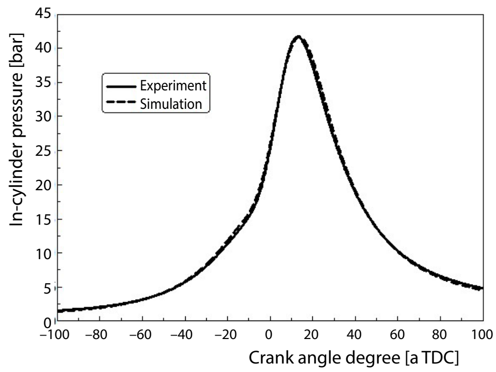

Figure 2. In-cylinder pressure comparison between experiment and simulation at 1400 rpm, 6 bar BMEP without cooled EGR under 60 °C coolant temperature

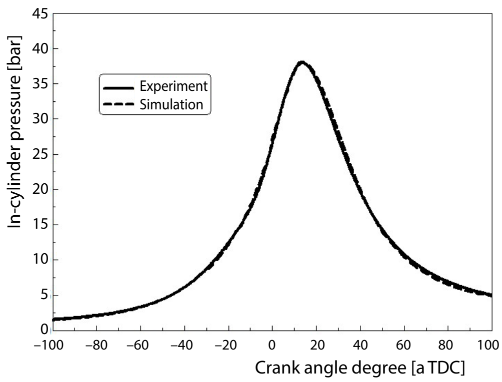

Figure 3. In-cylinder pressure comparison between experiment and simulation at 1400 rpm, 6 bar BMEP with 23% cooled EGR under 60 °C coolant temperature

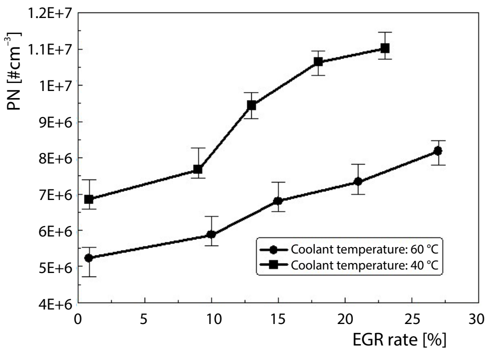

Figure 4. Effect of cooled EGR on PN emissions at 1400 rpm, 6 bar BMEP under 40 °C and 60 °C coolant temperatures

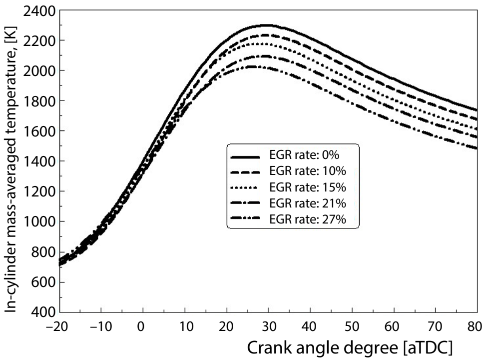

Figure 5. Effect of cooled EGR on in-cylinder mass-averaged temperature for SIDI operation at 1400 rpm, 6 bar BMEP and 60 °C coolant temperature conditions

lower temperature than the saturation temperature for most of the fuel species, resulting in the formation of fuel films once the fuel spray impinges onto piston surface, intake valves, and cylinder liner. For the spray-guided SIDI engine investigated here, where injector is central mounted in the combustion chamber, the fuel spray-piston impingement is the dominant reasons for the fuel films formation. These fuel films could form fuel rich areas due to insufficient evaporation and mixing, and generate diffusion-controlled flames during the following combustion, which is responsible for the high particle emissions. In addition, lower combustion chamber temperature intensifies the heat transfer losses from hot gases into cylinder walls, which reduces the post-flame oxidation rate of the particles formed during combustion. Therefore, when decreasing cold engine coolant temperature from 60 °C to 40 °C, more fuel films on the combustion chamber wall would be generated and the particle oxidation process would be further suppressed, resulting in higher PN emissions.

The addition of cooled EGR into engine further cools down the combustion chamber temperature at cold engine conditions. Figure 5 illustrates the effect of cooled EGR on in-cylinder mass-averaged temperature at 1400 rpm, 6 bar BMEP with 60 °C coolant temperature condition. It is shown that higher EGR level results in the lower combustion temperature ranging from 0 to 80 °CA, aTDC. This decrease in combustion temperature results from higher heat capacity and lower oxygen concentration. When increasing EGR ratio from 0 to 27%, peak combustion temperature is decreased from 2295 K to 2021 K. Decreased hot gases temperature will reduce combustion chamber temperature, leading to higher probability of generating fuel films on the piston surface. In addition, as EGR levels increase, in-cylinder oxygen concentration will decrease, which results in the decreased rate of particle oxidation.

In summary, decreasing engine coolant temperature and/or increasing cooled EGR at cold engine operation will generate higher PN emissions. The observed increase in particle emissions with lower engine coolant temperature and EGR at cold engine condition is believed to be resulted from more fuel films generated on the combustion chamber surface, and the suppressed particle oxidation process.

High-load warm-engine evaluation

The PN emissions behavior with increasing cooled EGR at 2200 rpm, 10 bar BMEP under warm engine operation is examined in fig. 6. By increasing the EGR rate to 17%, the PN emissions are shown to decrease by nearly 30%. This finding for the PN behaviors with cooled

EGR is different with the results shown in the above chapter, where engine is operated at low-load cold conditions. However, the finding is consistent with the work by Michael *et al*. [25], where 12% cooled EGR provides 6% reduction in PN emissions at high-load warm-engine operation (2000 rpm, 11 bar BMEP).

Compared to the cold-engine operation shown above, the piston temperature is higher at warm-engine operation. The impinged fuel on the piston will be evaporated much faster, therefore, the importance of spray-piston impingement in PN emission will be reduced. Moreover, a larger amount of fuel is required into the cylinder at high-load conditions, leading to more presence of locally fuel-rich mixture in the combustion chamber, and of liquid fuel around injector tip, which provide the ideal conditions for the formation of soot particles in the engine. Recent results in fundamental gasoline engine research have shown that the formation and oxidation of soot particles are highly dependent on temperature and oxygen concentration. The favorable conditions for soot emissions are the rich combustion with high temperature ranging from 1500 K to 2400 K, soot shows a bell-shaped dependence on reaction temperature with a peak around 1800 K [28]. On the higher temperature side of the peak, soot increases with temperature decreasing, and *vice versa* on the lower temperature side. Moreover, in-cylinder optical research in a central injection SIDI gasoline engine demonstrated that the injector diffusion flame associated with injector tip deposit, during and/or after the final phase of completion of the normal combustion event (between 20° and 80° crank angle after TDC), is a strong contributor to the particle emissions under warm engine operation [13].

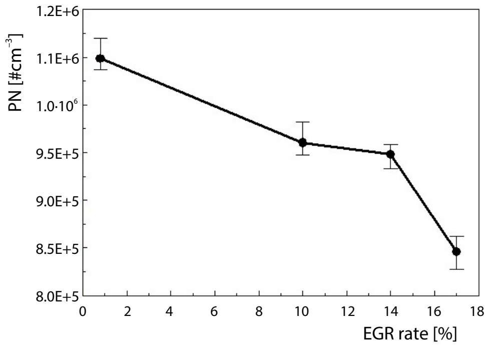

Figure 6. Effect of cooled EGR on PN emissions at 2200 rpm,10 bar BMEP under 90 °C coolant temperature condition

Figure 7 examines the effect of cooled EGR on in-cylinder mass-averaged temperature at 2200 rpm, 10 bar BMEP under the engine coolant temperature of 90 °C. It is found that the in-cylinder temperature decreases with cooled EGR during the crank angle ranging from 30 to 100 °CA, aTDC, where the injector diffusion flames and pool fires are expected to be occurred. In this crank angle range, the temperature decreases with EGR are located in the higher temperature side of the soot generation regions. Therefore, the cooled EGR may promote the particle formation. However, fig. 7 also shows that the cooled EGR increases the in-cylinder temperature during the crank angle ranging from –10 to 30 °CA, aTDC. This increase in combustion temperature is resulted from the earlier start of combustion achieved by advanced spark timing, which is realized due to the suppressed knock tendency with EGR increasing. The increased hot gases temperature will heat up the injector tip and piston surface, which will promote the fuel film evaporation process, and hence, suppress the particle formation

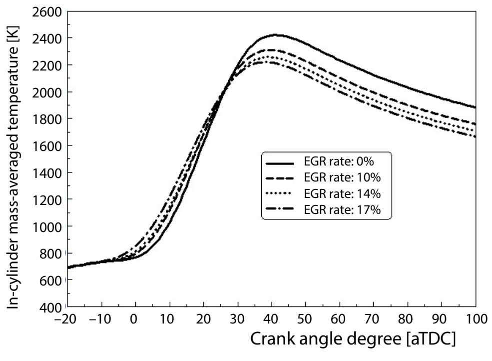

Figure 7. Effect of cooled EGR on in-cylinder mass-averaged temperature for SIDI operation at 2200 rpm, 10 bar BMEP under 90 °C coolant temperature condition

process. It has to be indicated that the further in-cylinder optical diagnostics research is necessary to investigate the in-cylinder distributions of soot and temperature so as to address this issue.

Conclusions

A boosted 1.4 L gasoline engine configured with central direct injection was used to explore the effect of cooled HP-EGR on particle emissions at low-load cold-engine and high-load warm-engine operation conditions. From this study, the following conclusions are made.

- At cold engine operation conditions, decreasing engine coolant temperature and/or increasing cooled EGR at low-load cold-engine operation will generate higher PN emissions. 60% higher PN emission is observed when adding 23% HP-EGR at 1400 rpm, 6 bar BMEP under 40 °C engine coolant temperature condition.
- The higher PN emission with HP-EGR and/or lower coolant temperature at low-load cold-engine operation is believed to be resulted from more fuel films generated on the combustion chamber surface, and the suppressed particle oxidation process.
- At high-load warm-engine operation, cooled EGR tends to decreases PN emissions. 30% lower PN emission is observed by 17% cooled EGR at 2200 rpm, 10 bar BMEP under 90 °C coolant temperature condition.
- The increased in-cylinder gas temperature before the injector tip flames and pool fires might be responsible for the observed lower PN when adding cooled EGR at high-load warm-engine operation.

Acronymes

aTDC – after top dead center
bTDC – before top dead center
BMEP – brake mean effective pressure
CAD – crank angle degree
CPC – condensation particle counter
EGR – exhaust gas recirculation
ET – evaporation tub
EVC – exhaust valve close
EVO – exaust valve open
HC – hydrocarbon
IVC – inlet valve closure
IVO – intake valve open
NEDC – new European driving cycle
PCF – particle pre-classifier
PDU – pre-dilution unit
PFI – port fuel injection
PN – particle number
PND – particle number diluter
rpm – round per minute
SIDI – spark ignition direct injection
SOF – soluble organic fraction
TDC – top dead center
TWC – three-way catalyst
VPR – volatile particle remover
VVT – variable valve timing
WLTC – worldwide harmonized light duty test cycle TWC three-way catalyst

References

[1] Ali, N., *et al*., Exhaust Gas Heat Recovery through Secondary Expansion Cylinder and Water Injection in an Internal Combustion Engine, *Thermal Science*, *21* (2017), 15, pp. 729-743
[2] Boretti, A., Towards 40% Efficiency with BMEP Exceeding 30 bar in Directly Injected, Turbocharged, Spark Ignition Ethanol Engines*, Energy Convers Manage*, *57* (2012), May, pp. 154-166
[3] Zaccardi, J., *et al*., Optimal Design for a Highly Downsized Gasoline Engine, SAE technical paper, 2009-01-1794, 2009
[4] Karnigstein, A., *et al*., Comparison of Advanced Turbocharging Technologies Under Steady-State and Transient Conditions, SAE technical paper, 2006-05-0364, 2006
[5] ***, United States Environmental Protection Agency (U. S. EPA), Light-Duty Automotive Technology, Carbon Dioxide Emissions, and Fuel Economy Trends: 1975 through 2010, U. S. EPA, Washington, D. C., 2010, EPA-420-R-10-023
[6] Stacy, D., *et al*., Vehicle Technologies Market Report 2015, Oak Ridge National Laboratory, Oak Ridge, Tenn., USA, 2016

[7] ***, The International Council on Clean Transportation, European Vehicle Market Statistics – Pocketbook 2014, http://eupocketbook.theicct.org, Jan., 2015
[8] Su, J., *et al*., Particulate Matter Emission Comparison of Spark Ignition Direct Injection (SIDI) and Port Fuel Injection (PFI) Operation of a Boosted Gasoline Engine, *Journal of Engineering for Gas Turbines and Power*, *136* (2014), 9, pp. 091513
[9] Price, P., *et al*., Particulate Matter and Hydrocarbon Emissions Measurements: Comparing First and Second Generation DISI with PFI in Single Cylinder Optical Engines, SAE technical paper, 2006-01-1263, 2006
[10] Velji, A., *et al*., Investigations of the Formation and Oxidation of Soot Inside a Direct Injection Spark Ignition Engine Using Advanced Laser-Techniques, SAE technical paper, 2010-01-0352, 2010
[11] Stevens, E., Steeper, R., Piston Wetting in an Optical DISI Engine: Fuel Films, Pool Fires, and Soot Generation, SAE technical paper, (2001), 2001-01-1203
[12] Konigstein, A., *et al*, Alternatives to Meet Future Particulate Emission Standards with a Boosted SIDI Engine, *Proceedings*, 24th Aachen Colloquium Automobile and Engine Technology, Aachen, Germany, 2015
[13] Berndorfer, A., *et al*., Diffusion Combustion Phenomena in GDi Engines Caused by Injection Process, SAE technical paper, 2013-01-0261, 2013
[14] Maier, A., *et al.,* Fuel-Independent Particulate Emissions in an SIDI Engine, SAE technical paper, 2015-01-1081, 2015
[15] Choi, K., *et al*., Effect of the Mixture Preparation on the Nanoparticle Characteristics of Gasoline Direct-Injection Vehicles, *Proc. Inst. Mech. Eng. D., J. Automob. Eng*, 226 (2012), 11, pp.1514-1524
[16] Piock, W., *et al*.,Strategies Towards Meeting Future Particulate Matter Emission Requirements in Homogeneous Gasoline Direct Injection Engines, SAE technical paper, 2011-01-1212, 2011
[17] Arash, N., *et al.* Decreasing the Emissions of a Partially Premixed Gasoline Fueled Compression Ignition Engine by Means of Injection Characteristics and Exhaust Gas Recirculation, *Thermal Science*, *15* (2011), 4, pp. 939-952
[18] Alger, T., *et al.,* Cooled Exhaust-Gas Recirculation for Fuel Economy and Emissions Improvement in Gasoline Engines, *Int. J. Engine Res.*, *12* (2011), 3, pp. 252-264
[19] Su, J., Xu, *et al*., Combined Effects of Cooled EGR and a Higher Geometric Compression Ratio on Thermal Efficiency Improvement of a Downsized Boosted Spark-Ignition Direct-Injection Engine, *Energy Conversion and Management*, *78* (2014), Feb., pp. 65-73
[20] Potteau, S., *et al*., Cooled EGR for a Turbo SI Engine to Reduce Knocking and Fuel Consumption, SAE technical paper, 2007-01-3978, 2007
[21] Alger, T., *et al.,* Synergies between High EGR Operation and GDI Systems, SAE technical paper, 2008-01-0134, 2008
[22] Abd-Alla G. H., Using Exhaust Gas Recirculation in Internal Combustion Engines: A Review, *Energy Convers Manage*, *43* (2002), 8, pp. 1027-1042
[23] Hedge, M., *et al*., Effect of EGR on Particle Emissions from a GDI Engine, SAE technical paper, 2011-01-0636, 2011
[24] Su, J., *et al*., Soot Emission Reduction Using Cooled EGR for a Boosted Spark-Ignition Direct-Injection (SIDI) Engine, *Proceedings*, 8th International Conference on Modeling and Diagnostics for Advanced Engine Systems, Fukuoka, Japan, 2012, pp. 23-26
[25] Winkler, M., *et al*., Low Pressure EGR for Downsized Gasoline Engines, *Proceedings*, 23rd Aachen Colloquium Automobile and Engine Technology, Aachen, Germany, 2014
[26] Ghojel, J. I., Review of the Development and Applications of the Wiebe Function: Attribute to the Contribution of Ivan Wiebe to Engine Research, *Int. J. Engine Res.*, *11* (2010), 4, pp. 297-312
[27] Verhelst, S., Sheppard, C. G. W., Multi-Zone Thermodynamic Modelling of Spark-Ignition Engine Combustion – An Overview, *Energy Convers Manage*, *50* (2009), 5, pp. 1326-1335
[28] Kopple, F., *et al*., Experimental Investigation of Fuel Impingement and Spray-Cooling on the Piston of a GDI Engine via Instantaneous Surface Temperature Measurements, SAE technical paper, 2014-01-1447, 2014

Paper submitted: February 7, 2018
Paper revised: March 25, 2018
Paper accepted: March 31, 2018